Valorization of Napier grass via intermediate pyrolysis: Optimization using response surface methodology and pyrolysis products characterization

MOHAMMED, Isah Yakub, ABAKR, Yousif Abdalla, YUSUP, Suzana and KABIR, Feroz <http://orcid.org/0000-0002-3121-9086>

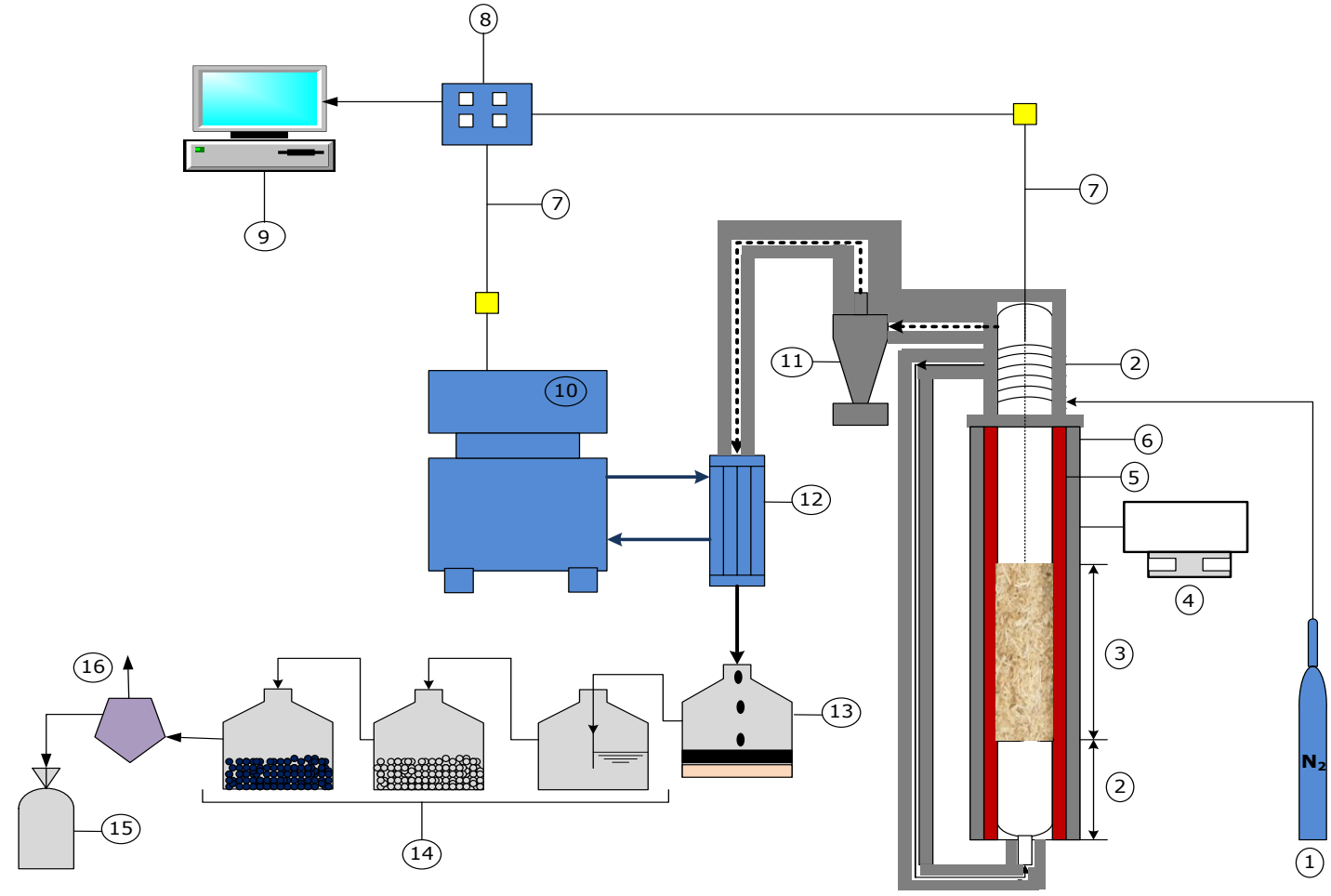

Fig. 1. Experimental set-up. (1) Nitrogen cylinder, (2) nitrogen preheating sections, (3) pyrolysis section, (4) furnace controller, (5) heater, (6) insulator, (7) thermocouples, (8) data logger, (9) computer, (10) water chiller, (11) cyclone, (12) condenser, (13) bio-oil collector, (14) gas scrubber, (15) gas sampling bag, (16) gas venting

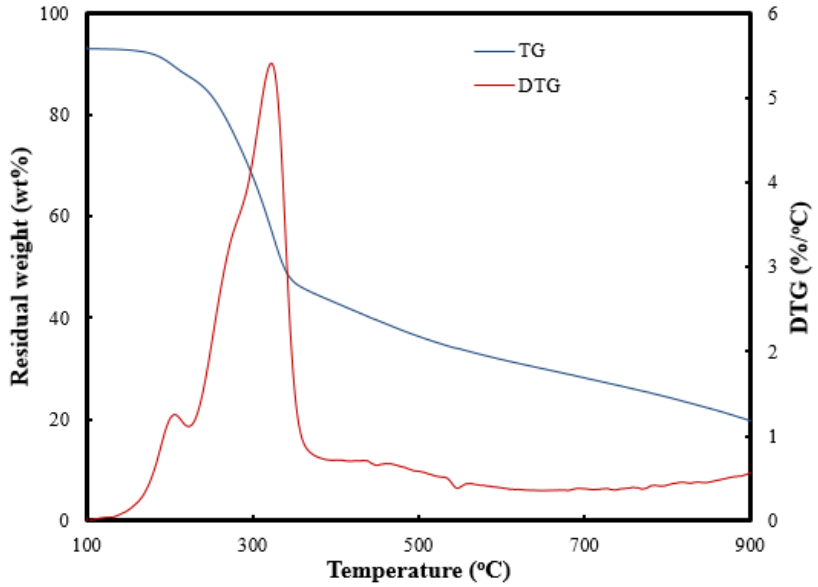
TG
DTG
Residual weight (wt%)
DTG (%/°C)
Temperature (°C)
100
80
60
40
20
0
6
5
4
3
2
1
0
100
300
500
700
900

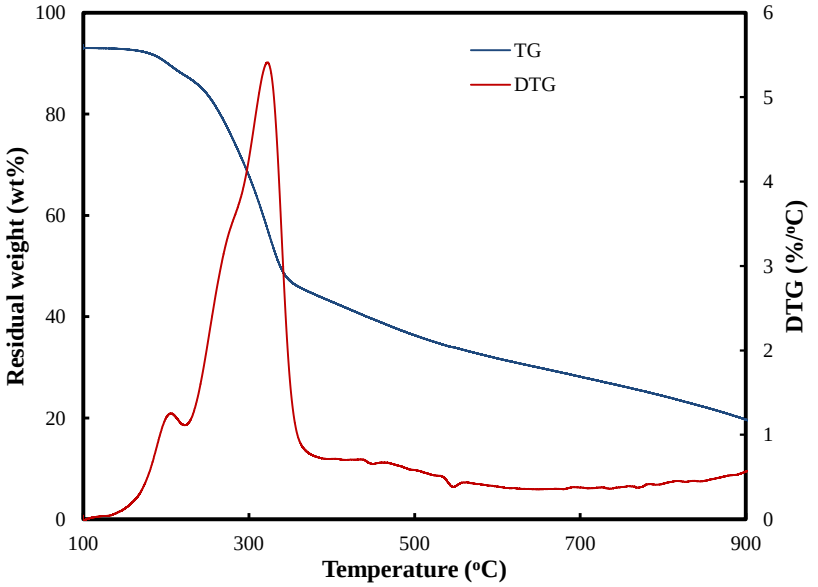
TG
DTG
Residual weight (wt%)
DTG (%/°C)
Temperature (°C)
100
80
60
40
20
0
6
5
4
3
2
1
0
100
300
500
700
900

Fig. 2. Thermogravimetric profile of Napier grass stem (TG and DTG). Sample particle size (0.2mm); Nitrogen flow (20mL/min); heating rate (10^{o}C/min)

Formatted: Indent: Left: 0 cm, Right: 0 cm

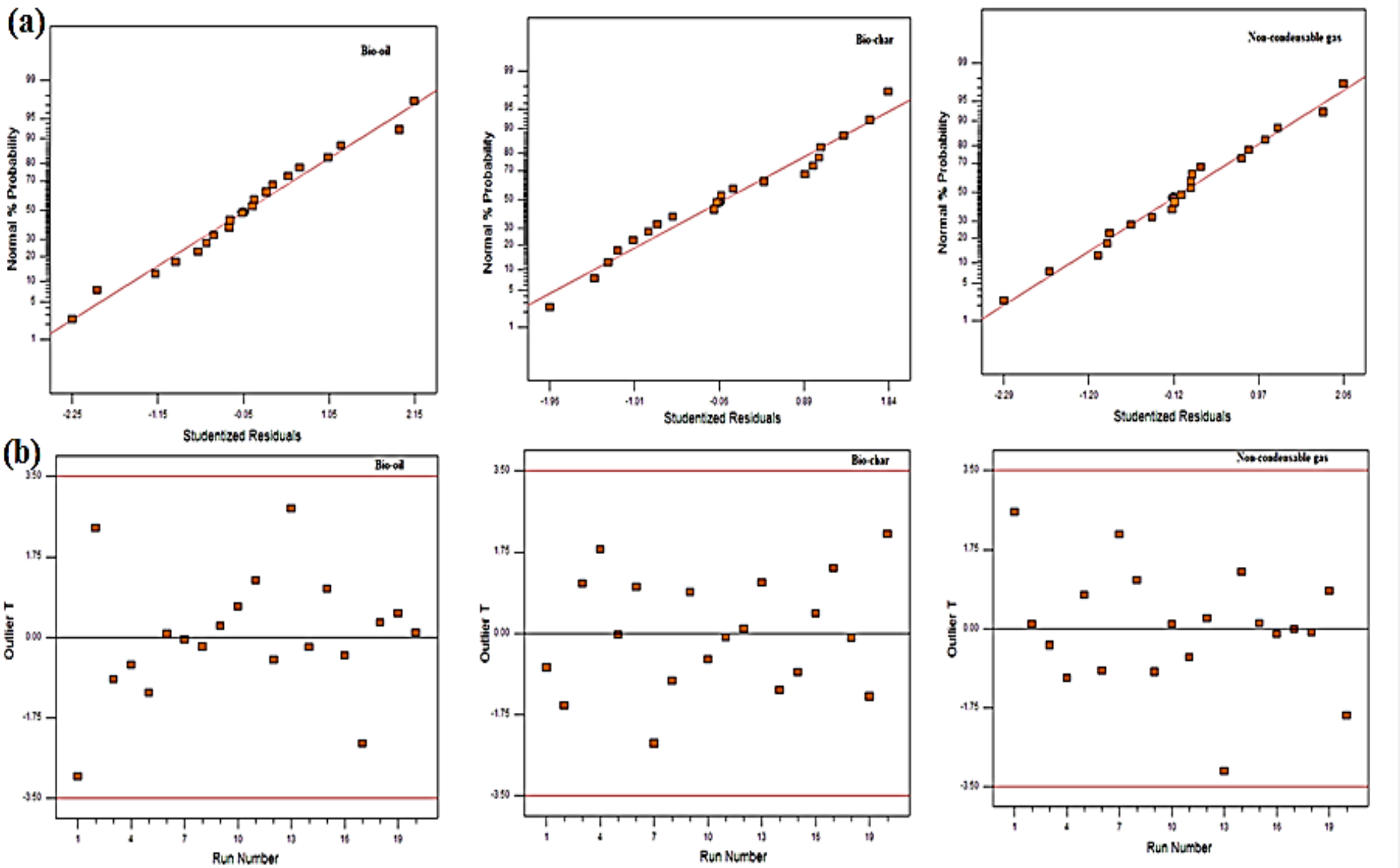

Fig. 3. Diagnostics of models (a) Normal % probability versus studentized residuals (b) Outliers T versus run number

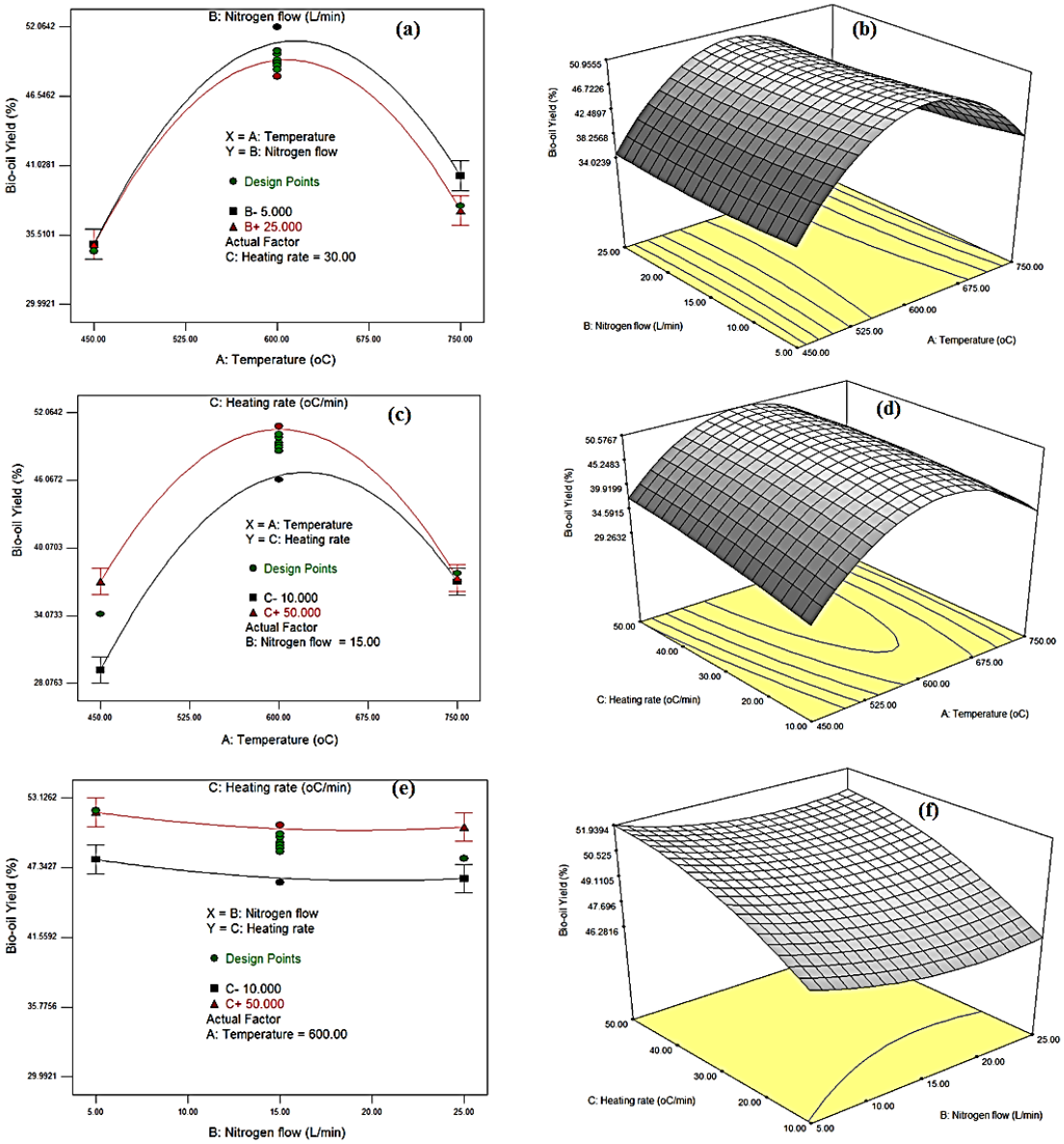

Fig. 4. Interaction graphs and the corresponding surface response plots for the combined effects of process variables on bio-oil yield. (a) and (b) effect of nitrogen flow and temperature at 30^{o}C/min; (c) and (d) effect of heating rate and temperature at 15L/min N_2; (e) and (f) effect heating rate and nitrogen flow at 600^{o}C

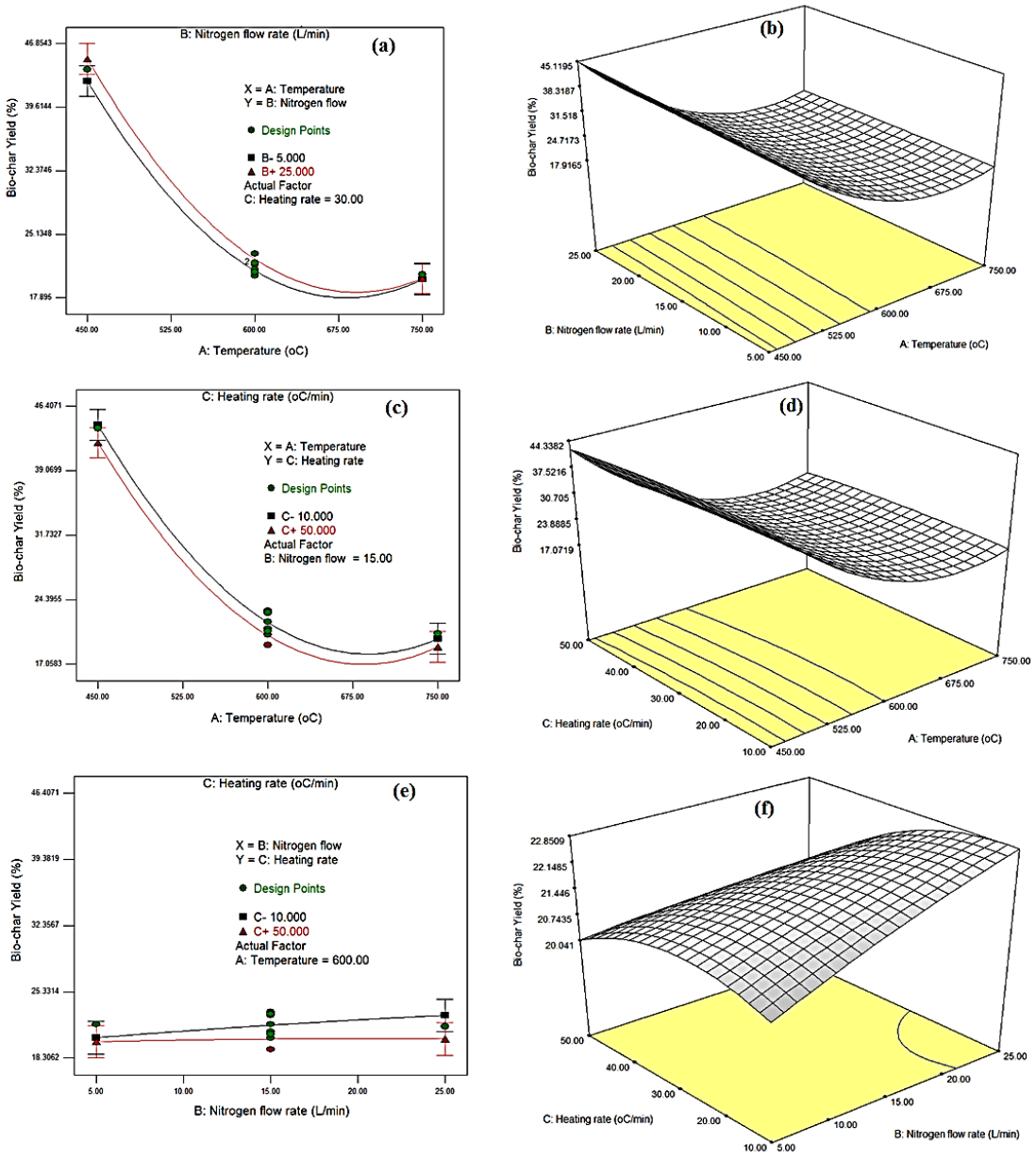

Fig. 5. Interaction graphs and the corresponding surface response plots for the combined effects of process variables on bio-char yield. (a) and (b) effect of nitrogen flow and temperature at 30^{o}C/min; (c) and (d) effect of heating rate and temperature at 15L/min N_2; (e) and (f) effect heating rate and nitrogen flow at 600^{o}C

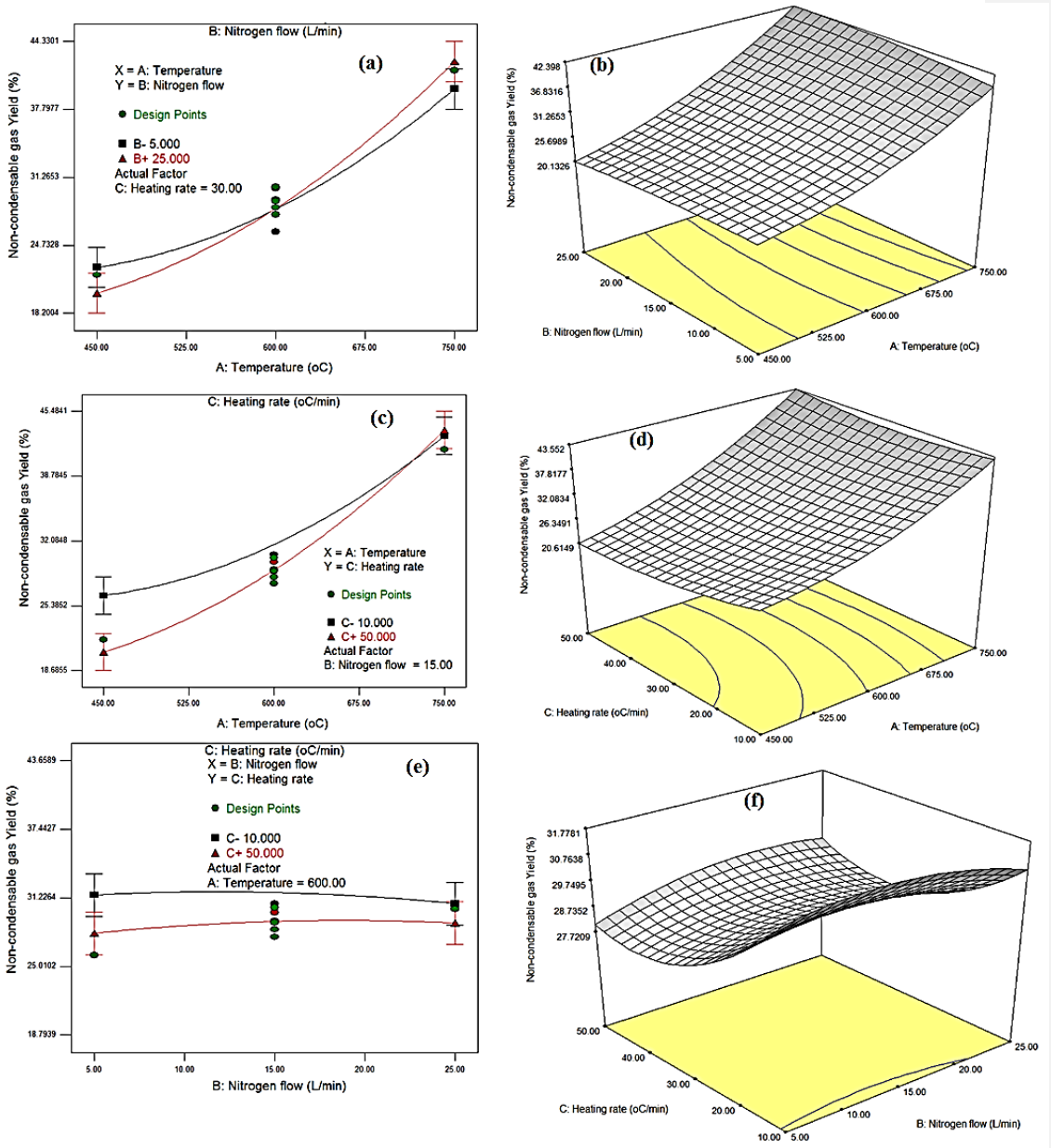

Fig. 6. Interaction graphs and the corresponding surface response plots for the combined effects of process variables on non-condensable gas yield. (a) and (b) effect of nitrogen flow and temperature at 30^{o}C/min; (c) and (d) effect of heating rate and temperature at 15L/min N_2; (e) and (f) effect heating rate and nitrogen flow at 600^{o}C

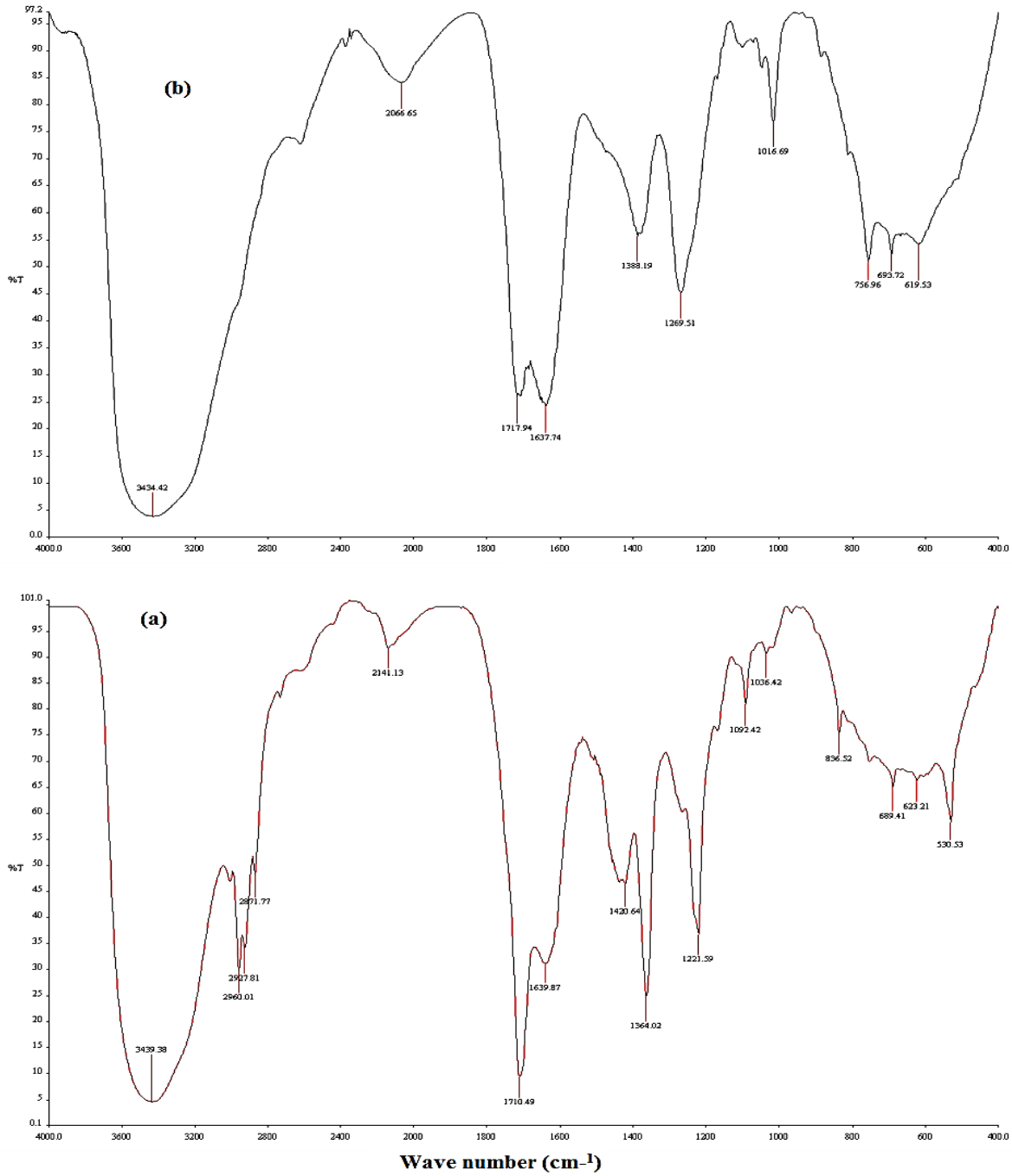

Fig. 7. Averaged FTIR spectra (auto-smoothed and auto-baseline corrected) of bio-oil obtained at optimized condition (a) organic phase; (b) aqueous phase

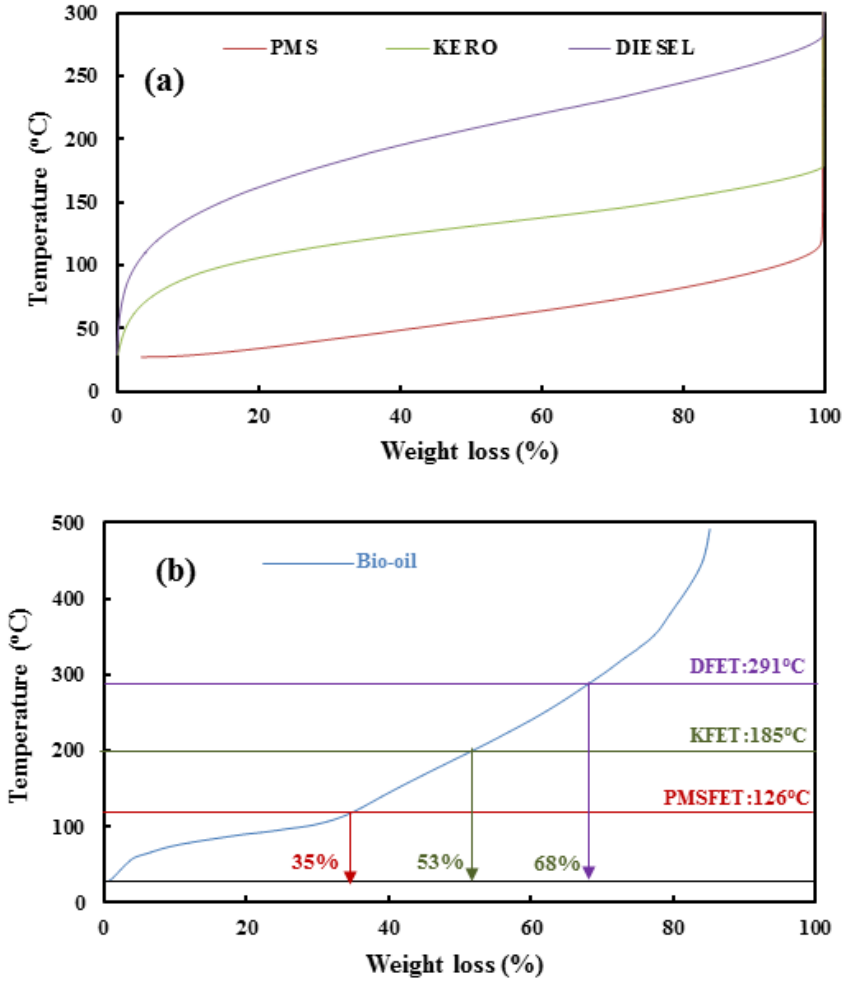

Fig. 8. Simulated Distillation using TGA. (a) Premium motor sprit-PMS, kerosene and diesel (b) organic phase bio-oil. DFET, KFET and PMSFET: diesel, kerosene and PMS final evaporation temperature.

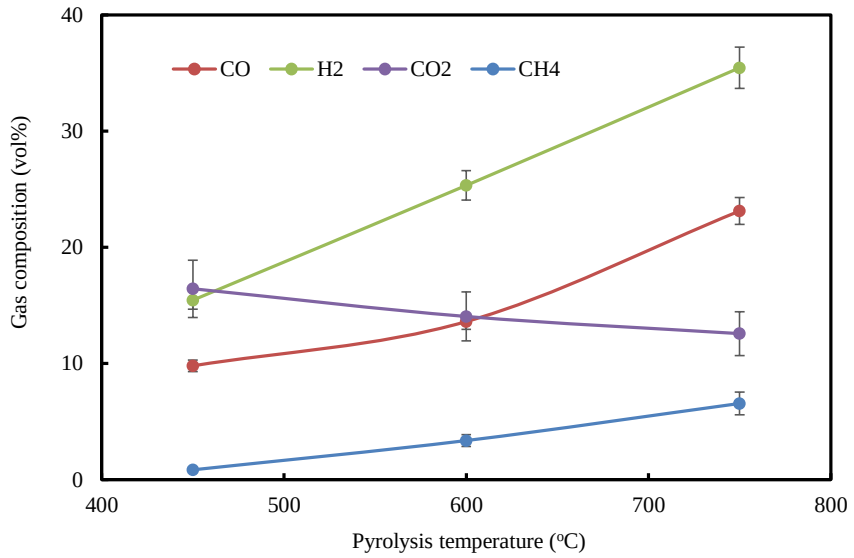

Fig. 9. Composition of non-condensable gas collected (N_2 free basis) at 50 °C/min and 5 L/min N_2 at different pyrolysis temperature. Values are the means (n = 2) ± SD

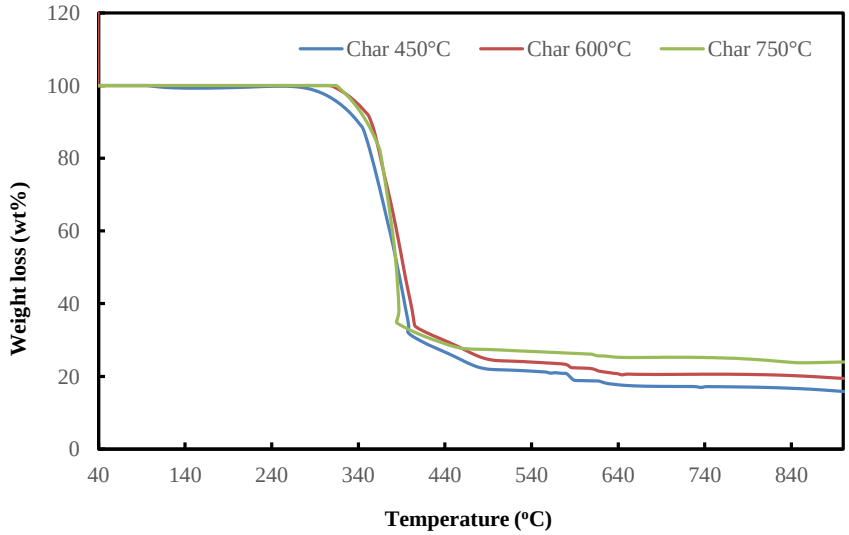

Fig. 10. Combustion profile of NGS bio-char produced at different pyrolysis temperature. Condition: 10 mg sample, 50 mL/min oxygen and 10 °C/min heating rate

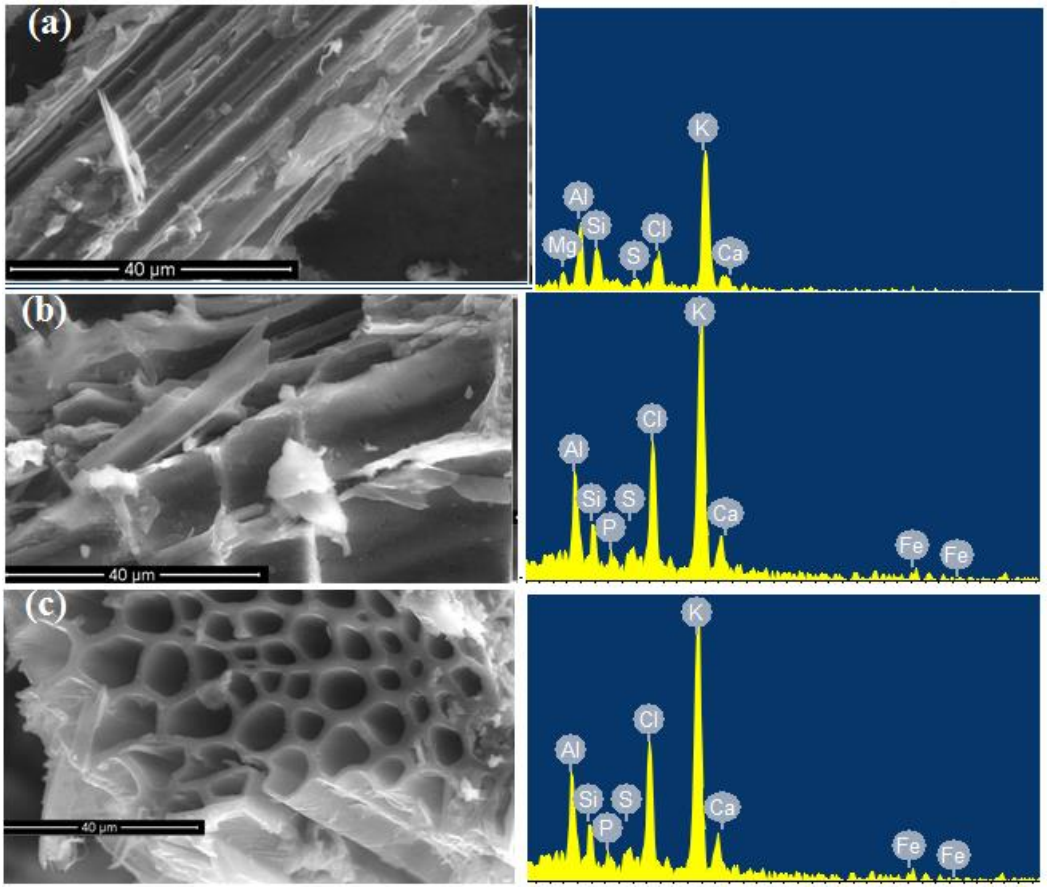

Fig. 11. SEM-EDX of biochar obtained at (a) 450 ^{o}C, (b) 600 ^{o}C and (c) 750 ^{o}C from NGS biomass